COHERENCE FUNCTION ESTIMATION WITH A DERIVATIVE CONSTRAINT FOR POWER GRID OSCILLATION DETECTION

Mohammadreza Ghorbaniparvar, Ning Zhou, Xiaohua Li

Department of Electrical and Computer Engineering
State University of New York at Binghamton
Binghamton, NY 13902
{mghorba1,ningzhou,xli}@binghamton.edu

ABSTRACT

Oscillation is one of the leading stability concerns in complex power systems. Detecting oscillations timely and accurately is vital for a power grid operator to take effective remedial reactions to stabilize the power system. This paper uses the minimum variance distortionless response (MVDR) method to estimate the magnitude squared coherence function for oscillation detection. A derivative constraint is integrated into the MVDR method, which can greatly mitigate the "blind spots" problem of the conventional MVDR method. The phenomenon of the "blind spots" and the mitigation performance of the new technique are analyzed. Simulations based on power system models are conducted to demonstrate that the new technique can effectively avoid the "blind spots" and thus increase the accuracy of oscillation detection in power systems.

***Index Terms*—** power system, oscillation, magnitude squared coherence, MVDR, Capon method, spectrum.

1. INTRODUCTION

Oscillations with growing amplitudes can cause serious problems to power systems such as system break-ups and large-scale outages [1][2]. Sustained oscillations can negatively affect the life expectancy of equipment [3]. To ensure the stability and reliability of a power grid, it is important to detect the oscillations timely and accurately in their early stages.

Oscillations in a power grid can be categorized into free and forced oscillations. Free oscillations are the results of internal interaction among the system equipment, while forced oscillations are caused by external inputs. Over the last twenty years, many methods have been proposed to study the free oscillations [4]. Recently, forced oscillations have gained a lot of attention because they happen more frequently in power grids [5] [6].

One of the early studies on forced oscillations goes back to 1966 when Ness proposed a method to study the system response to large cyclic load variations [7]. Using the widely deployed phasor measurement units (PMUs), a hybrid dynamic simulation method is proposed in [8] to locate forced oscillations. An energy based method is introduced in [9] to locate the disturbance source. Follum et al. [10] proposes to detect the oscillations before locating them. Zhou in [11] proposed a coherence method to detect the oscillations. This method is further developed in [12] into a self-coherence method using only one channel of data. To quantify the detection results of the self-coherence method, a bootstrap-based threshold is given in [13]. A cross-coherence method is developed in [14] to use multiple channel data.

These coherence methods are based on the coherence spectrum, a.k.a, the magnitude squared coherence (MSC) function, for oscillation detection [15][16]. The MSC function can be estimated by many different spectral estimation methods such as the Welch's method [17] and the ARMA method [18]. It is shown in [14] that the minimum variance distortionless response (MVDR) method, also known as the Capon method [19], has many advantages such as real-time applicability, multi-channel data adaptability, low risk of false alarm, and high estimation accuracy. It can achieve smaller variance and higher accurate than the Welch's method and the ARMA method.

However, one major drawback of the MVDR method is that the estimated MSC does not cover all the frequencies. There are many "blind spots" where the MSC values are always small or zero. In this paper, we analyze the "blind spots" phenomenon and show that this problem can be mitigated effectively by simply adding a derivative constraint into the MVDR optimization.

This paper is organized as follows. In Section 2, the oscillation problem in power system and the application of the MSC function are introduced. In Section 3, we develop the new MVDR method with a derivative constraint. Simulations are conducted in Section 4 and conclusions are presented in Section 5.

2. OSCILLATION DETECTION IN POWER SYSTEMS

Based on [1], a power system's dynamic response to small motions can be described as

$$\dot{\mathbf{x}}(t) = \mathbf{A}\mathbf{x}(t) + \mathbf{b}_1 f(t) + \sum_{m=1}^{M} \mathbf{b}_{2m} q_m(t) \tag{1}$$

where $\mathbf{A}$ is the state transition matrix,$\mathbf{x}(t)$ is the $N \times 1$ dimensional system state vector, t is time, $f(t)$ is the forced oscillations, and $q_m(t)$ are noises.

Because the frequency of the steady-state responses to forced oscillations will remain the same, to simplify the study of oscillation detection, we can just use a simplified version of the power system response that carries a forced oscillation only, i.e.,

$$x(t) = f(t) + q(t), \tag{2}$$

where the forced oscillation $f(t)$ is modeled as a sinusoidal signal.

With the data $x(t)$, we need to detect the frequency of $f(t)$ timely and accurately, even in extremely large noise. Coherence spectrum is one of the promising ways for power system oscillation detection. For two discrete-time signals $x_1(n)$ and $x_2(n)$, the coherence spectrum (MSC function) is defined as

$$\gamma^2_{x_1x_2}(\omega) = \frac{|S_{x_1x_2}(\omega)|^2}{S_{x_1}(\omega)S_{x_2}(\omega)}, \tag{3}$$

where $S_{x_1x_2}(\omega)$ is the cross-spectrum between the two signals [20], while $S_{x_1}(\omega)$ and $S_{x_2}(\omega)$ are the power spectrum density (self-spectrum) of the two signals. Note that $x_1(n)$ and $x_2(n)$ can be two sampled signal components of $\mathbf{x}(t)$ based on (1). They can also be $x(n)$ and its delayed version $x(n-\tau)$ based on (2) when only one channel of data is available [12].

The MVDR method for MSC function estimation is based on the filter bank principle. Let the kth sub-filter of the filter bank be $\mathbf{w}_k = [w_{k,0}, \cdots, w_{k,L-1}]^H$ where $(\cdot)^H$ denotes conjugate transpose. For the input signal $x(n)$, the filter output is $y_k(n) = \mathbf{w}_k^H \mathbf{x}(n)$, where $\mathbf{x}(n) = [x(n), \cdots, x(n-L+1)]^T$ and $(\cdot)^T$ denotes transpose. The power of the output signal is

$$E\{|y_k(n)|^2\} = E\{|\mathbf{w}_k^H \mathbf{x}(n)|^2\} = \mathbf{w}_k^H \mathbf{R}_x \mathbf{w}_k \tag{4}$$

where $E\{.\}$ is expectation and $\mathbf{R}_x = E\{\mathbf{x}(n)\mathbf{x}^H(n)\}$ is the covariance matrix of the input signal $x(n)$ (which is assumed zero-mean).

To find the power spectrum density $S_x(\omega_k)$ of the signal $x(n)$ at frequency ω_k, we just need to solve the linearly constrained minimum variance (LCMV) optimization

$$\begin{cases} \min\limits_{\mathbf{w}_k} & S_x(\omega_k) = \mathbf{w}_k^H \mathbf{R}_x \mathbf{w}_k \\ \text{s.t.} & \mathbf{c}_k^H \mathbf{w}_k = 1 \end{cases} \tag{5}$$

with the constraint vector $\mathbf{c}_k = [1, e^{j\omega_k}, \cdots, e^{j\omega_k(L-1)}]^T/\sqrt{L}$. The optimal solution to (5) is

$$\mathbf{w}_{k,opt} = \frac{\mathbf{R}_x^{-1}\mathbf{c}_k}{\mathbf{c}_k^H \mathbf{R}_x^{-1} \mathbf{c}_k} \tag{6}$$

and the power spectrum density (self-spectrum) of $x(n)$ at frequency ω_k is

$$S_x(\omega_k) = \mathbf{w}_{k,opt}^H \mathbf{R}_x \mathbf{w}_{k,opt} = \frac{1}{\mathbf{c}_k^H \mathbf{R}_x^{-1} \mathbf{c}_k}. \tag{7}$$

Using the filter bank, we can find the power spectrum density at a list of discrete frequencies ω_k, $k = 0, \cdots, K-1$. Note that we have K subfilters, each subfilter has order L. If $K = L$ and the frequency $\omega_k = 2\pi k/K$, then the filters forms the FFT matrix. On the other hand, we can make $K > L$ to increase resolution.

To estimate the MSC function (3) of $x(n)$, we let $x_1(n) = x(n)$ and $x_2(n) = x(n-\tau)$ for certain large enough delay τ. Then we apply (7) to calculate $S_{x_1}(\omega_k) = \frac{1}{\mathbf{c}_k^H \mathbf{R}_{x_1}^{-1}\mathbf{c}_k}$ and $S_{x_2}(\omega_k) = \frac{1}{\mathbf{c}_k^H \mathbf{R}_{x_2}^{-1}\mathbf{c}_k}$. In addition, let $y_{1,k}(n) = \mathbf{w}_{1,k}^H \mathbf{x}_1(n)$ and $y_{2,k}(n) = \mathbf{w}_{2,k}^H \mathbf{x}_2(n)$ be the outputs of the two sub-filters with inputs $x_1(n)$ and $x_2(n)$, respectively. The cross-spectrum is

$$S_{x_1x_2}(\omega_k) = E\{y_{1,k}(n)y_{2,k}^H(n)\} = \mathbf{w}_{1,k}^H \mathbf{R}_{x_1x_2} \mathbf{w}_{2,k} \tag{8}$$

where $\mathbf{R}_{x_1x_2} = E\{x_1(n)x_2^H(n)\}$ is the cross-correlation matrix. Based on (6), we can obtain

$$S_{x_1x_2}(\omega_k) = \frac{\mathbf{c}_k^H \mathbf{R}_{x_1}^{-1} \mathbf{R}_{x_1x_2} \mathbf{R}_{x_2}^{-1} \mathbf{c}_k}{(\mathbf{c}_k^H \mathbf{R}_{x_1}^{-1}\mathbf{c}_k)(\mathbf{c}_k^H \mathbf{R}_{x_2}^{-1}\mathbf{c}_k)}. \tag{9}$$

Therefore, the MSC function (3) can be calculated as

$$\gamma^2_{x_1x_2}(\omega_k) = \frac{\left|\mathbf{c}_k^H \mathbf{R}_{x_1}^{-1} \mathbf{R}_{x_1x_2} \mathbf{R}_{x_2}^{-1} \mathbf{c}_k\right|^2}{\left(\mathbf{c}_k^H \mathbf{R}_{x_1}^{-1}\mathbf{c}_k\right)\left(\mathbf{c}_k^H \mathbf{R}_{x_2}^{-1}\mathbf{c}_k\right)}. \tag{10}$$

Comparing $\gamma^2_{x_1x_2}(\omega_k)$ with the noise background, we can determine whether there is an oscillation with the frequency ω_k in the signal $x(n)$ [12].

3. DERIVATIVE CONSTRAINED MVDR

While the MVDR has a number of advantages for power grid oscillation detection, it suffers from the problem of "blind spots". This is mainly because the constraints $\mathbf{c}_k$ are designed for a list of fixed discrete frequencies only and the frequency gap is usually larger than the power grid oscillation frequency.

Proposition 1. Assume the signal $x(n)$ is dominated by a single frequency $\tilde{\omega}$, i.e., $x(n) = e^{j\tilde{\omega}n} + z(n) + q(n)$ where $E\{|z(n)|^2\} \ll 1$ and noise power $\sigma_q^2 \ll 1$. If $\tilde{\omega} \neq \omega_k$ for all $k = 0, \cdots, K-1$, then the MVDR method gives $\gamma^2_{x_1x_2}(\omega_k) \approx 0$.

Proof. Applying the signal $x(n)$ in the optimization (5), we can get $\mathbf{w}_k^H \mathbf{R}_x \mathbf{w}_k = \mathbf{w}_k^H(\tilde{\mathbf{c}}\tilde{\mathbf{c}}^H + E\{\mathbf{z}(n)\mathbf{z}^H(n)\} + E\{\mathbf{q}(n)\mathbf{q}^H(n)\})\mathbf{w}_k \approx |\tilde{\mathbf{c}}^H \mathbf{w}_k|^2 + \sigma_q^2\|\mathbf{w}_k\|^2$, where $\tilde{\mathbf{c}} = [1, e^{j\tilde{\omega}}, \cdots, e^{j\tilde{\omega}(L-1)}]^T$. In case the noise power σ_q^2 is small enough, we can easily see that

$$\begin{bmatrix} \mathbf{c}_k^H \\ \tilde{\mathbf{c}}^H \end{bmatrix} \mathbf{w}_{k,opt} = \begin{bmatrix} 1 \\ 0 \end{bmatrix}. \tag{11}$$

This means that $S_x(\omega_k) = \mathbf{w}_{k,opt}^H \mathbf{R}_x \mathbf{w}_{k,opt} \approx \sigma_q^2\|\mathbf{w}_{k,opt}\|^2$.

Therefore, the sub-filter outputs $y_{1,k}(n)$ and $y_{2,k}(n)$ are just noises $q(n)$ and $q(n-\tau)$, respectively. This means $S_{x_1x_2}(\omega_k) \approx 0$ if $\tau > L$. Hence $\gamma^2_{x_1x_2}(\omega_k) \approx 0$. ■

Since the oscillation frequency may be different from any ω_k, Proposition 1 indicates that the MVDR method will gives $\gamma^2_{x_1x_2}(\omega_k) \approx 0$ for all k. In this case, the oscillation can not be detected timely and accurately. This is the "blind spots" phenomenon.

Increasing K can mitigate somewhat the "blind spots" problem. Intuitively, this makes $\tilde{\mathbf{c}}/\sqrt{L}$ closer to $\mathbf{c}_k$ for some k. Since $\|1 - \tilde{\mathbf{c}}^H/\sqrt{L}\mathbf{w}_{k,opt}\| = \|(\mathbf{c}_k^H - \tilde{\mathbf{c}}^H/\sqrt{L})\mathbf{w}_{k,opt}\| \leq \|\mathbf{c}_k^H - \tilde{\mathbf{c}}^H/\sqrt{L}\|\|\mathbf{w}_{k,opt}\|$, we see that $\tilde{\mathbf{c}}^H/\sqrt{L}\mathbf{w}_{k,opt} \to 1$. More accurately, from $\mathbf{R}_x \approx \tilde{\mathbf{c}}\tilde{\mathbf{c}}^H + \sigma_q^2\mathbf{I}$, where $\mathbf{I}$ is the identify matrix, using the matrix inversion lemma, we can readily derive $S_x(\omega_k) = \sigma_q^2/(1 - |\mathbf{c}_k^H\tilde{\mathbf{c}}|^2/(\sigma_q^2 + L))$. If $K = L = 256$, then we have $S_x(\omega_k) \approx 1.3\sigma_q^2$ for $\tilde{\omega}$ in the middle of ω_k and ω_{k+1}. This means a "blind slot" since the noise floor is σ_q^2. If $K = 2L = 256$, then $S_x(\omega_k) \approx 5\sigma_q^2$. This provides some relief from "blind spot" because there are some signal contents in filter output $y_{1,k}(n)$ and $y_{2,k}(n)$.

Nevertheless, a more effective approach of mitigating the "blind spots" problem is to simply add a derivative constraint to the LCMV optimization (5) to resolve this problem. Specifically, we set the first-order derivative of $\mathbf{c}_k$ with respect to the frequency ω_k to be zero as an addition constraint. By adding the constraint of the derivative, the amplitude response of the filter is forced to be flat at ω_k, which can mitigate the "blind spots" problem in the resulting spectra.

The new constraint can be stated as

$$\mathbf{C}_k^H \mathbf{w}_k = \mathbf{h} \tag{12}$$

where

$$\mathbf{C}_k = \begin{bmatrix} \mathbf{c}_k & \frac{d\mathbf{c}_k}{d\omega_k} \end{bmatrix}, \qquad \mathbf{h} = \begin{bmatrix} 1 \\ 0 \end{bmatrix}, \tag{13}$$

and $d\mathbf{c}_k/d\omega_k = [0, je^{j\omega_k}, \cdots, j(L-1)e^{j(L-1)\omega_k}]^T/\sqrt{L}$.

Proposition 2. With the new LCMV optimization

$$\begin{cases} \min\limits_{\mathbf{w}_k} & S_x(\omega_k) = \mathbf{w}_k^H \mathbf{R}_x \mathbf{w}_k \\ \text{s.t.} & \mathbf{C}_k^H \mathbf{w}_k = \mathbf{h} \end{cases} \tag{14}$$

we can calculate the MSC function as

$$\gamma^2_{x_1x_2}(\omega_k) = \frac{\left|\mathbf{h}^H \boldsymbol{\zeta}_{1,k} \mathbf{C}_k^H \mathbf{R}_{x_1}^{-1} \mathbf{R}_{x_1x_2} \mathbf{R}_{x_2}^{-1} \mathbf{C}_k \boldsymbol{\zeta}_{2,k} \mathbf{h}\right|^2}{(\mathbf{h}^H \boldsymbol{\zeta}_{1,k} \mathbf{h})(\mathbf{h}^H \boldsymbol{\zeta}_{2,k} \mathbf{h})} \tag{15}$$

where the 2×2 matrices $\boldsymbol{\zeta}_{i,k} = (\mathbf{C}_k^H \mathbf{R}_{x_i}^{-1} \mathbf{C}_k)^{-1}$, $i = 1, 2$.

Proof. For the general LCMV optimization (14), using the standard Lagrange multiplier method, we minimize

$$\min \quad J = \mathbf{w}_k^H \mathbf{R}_x \mathbf{w}_k + \mathrm{Re}\{\boldsymbol{\lambda}^H (\mathbf{C}_k^H \mathbf{w}_k - \mathbf{h})\} \tag{16}$$

where $\boldsymbol{\lambda}$ is the Lagrange multiplier vector and $\mathrm{Re}\{\cdot\}$ takes the real part. From $\partial J/\partial \mathbf{w}_k = \mathbf{w}_k^H \mathbf{R}_x + \boldsymbol{\lambda}^H \mathbf{C}_k^H = \mathbf{0}$, we obtain $\mathbf{w}_k^H = -\boldsymbol{\lambda}^H \mathbf{C}_k^H \mathbf{R}_x^{-1}$. Substituting $\mathbf{w}_k^H$ back into the constraint in (14), we can obtain $\boldsymbol{\lambda}^H = -\mathbf{h}^H (\mathbf{C}_k^H \mathbf{R}_x^{-1} \mathbf{C}_k)^{-1}$. Therefore, the optimal solution is

$$\mathbf{w}_{k,opt} = \mathbf{R}_x^{-1} \mathbf{C}_k (\mathbf{C}_k^H \mathbf{R}_x^{-1} \mathbf{C}_k)^{-1} \mathbf{h}. \tag{17}$$

Substituting $\mathbf{w}_{k,opt}$ into (14), the self-spectrum of $x_i(n)$, $i = 1, 2$, is

$$S_{x_i}(\omega_k) = \mathbf{h}^H (\mathbf{C}_k^H \mathbf{R}_{x_i}^{-1} \mathbf{C}_k)^{-1} \mathbf{h} = \mathbf{h}^H \boldsymbol{\zeta}_{i,k} \mathbf{h}. \tag{18}$$

Following (9)(10), we can derive the cross-spectrum of $x_1(n)$ and $x_2(n)$ as

$$S_{x_1x_2}(\omega_k) = \mathbf{h}^H \boldsymbol{\zeta}_{1,k} \mathbf{C}_k^H \mathbf{R}_{x_1}^{-1} \mathbf{R}_{x_1x_2} \mathbf{R}_{x_2}^{-1} \mathbf{C}_k \boldsymbol{\zeta}_{2,k} \mathbf{h}. \tag{19}$$

Substituting (18) and (19) into (3), we can get the MSC function (15). ■

To show that the new technique greatly mitigates the "blind spots" problem, consider again the signal $x(n)$ dominated by the single frequency $\tilde{\omega}$. Exploiting the matrix inversion lemma and the property of 2×2 inverse matrix, we can readily derive $S_x(\omega_k) = G\sigma_q^2/(\|\mathbf{d}\|^2 - |\mathbf{d}^H \tilde{\mathbf{c}}|^2/(\sigma_q^2 + L))$, where $\mathbf{d} = d\mathbf{c}_k/d\omega_k$ and G is a constant. If $K = L = 256$, then we have $S_x(\omega_k) \approx 4\sigma_q^2$ for $\tilde{\omega}$ in the middle of ω_k and ω_{k+1}. The "blind spot" is mitigated. If $K = 2L = 256$, then $S_x(\omega_k) \approx \sigma_q^2 + 1$, which is dominated by the oscillation frequency, and there is no obvious "blind spot" anymore.

With the PMU signal $x(n)$, we can calculate the MSC function according to (15) for each frequency ω_k. If $\omega_k = 2\pi k/K$, $k = 0, \cdots, K-1$, then we can exploit FFT for efficient calculation.

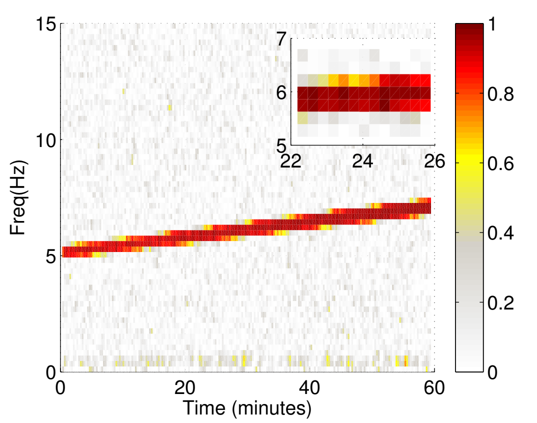

Fig. 1. MSC function of $\gamma^2_{x_1x_2}$ estimated by the Welch's method.

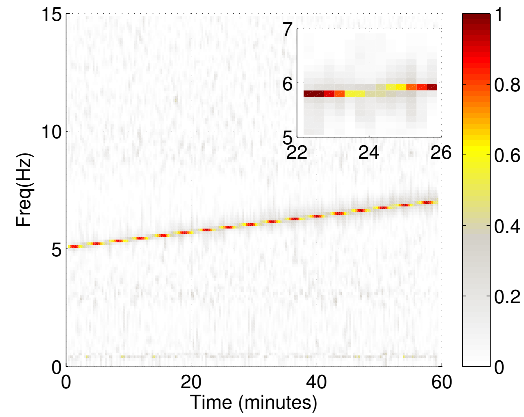

Fig. 2. MSC function of $\gamma^2_{x_1x_2}$ estimated by the generalized MVDR method.

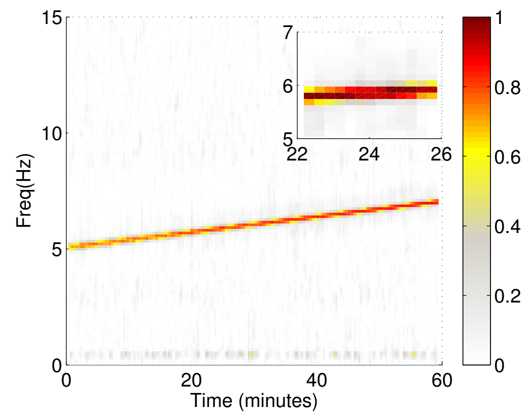

Fig. 3. MSC function of $\gamma^2_{x_1x_2}$ estimated by the proposed MVDR method with derivative constraints.

4. SIMULATIONS

We have conducted extensive simulations to evaluation the proposed derivative constrained MVDR method and compare it with the Welch method [17] and the Generalized MVDR method [19].

4.1. A simple example of chirp signal

First, we use a simple chirp signal to evaluate the performance of MSC estimation, in particular the "blind spots". The chirp signal $x(t) = \sqrt{2}\sin(2\pi f_0(t - t_0) + k\pi(t - t_0)^2 + \phi_i) + q(t)$ has instantaneous frequency changing from f_0 to f_1. At $t_0 = 0$, the chirp signal's power is concentrated at $f_0 = 5$Hz. Then, the frequency linearly increases at the rate of $k = (f_1 - f_0)/(t_1 - t_0) = 0.033$ Hz/min. Eventually, chirp signal's power at the 60^{th} minute is concentrated at $f_1 = 7$ Hz. Simulation data is generated for 60 minutes with sampling rate of 30 samples/s. We use a low-pass filter $G(s)$ to filter the Gaussian white noise to mimic the colored ambient noise $q(t)$. The standard deviation (std) of the ambient noise is modified to make the signal to noise ratio (SNR) -10 dB.

The initial setup of the Welch's method is $N = 1024, L = 128$, 50% overlapping and Hamming window. The initial set up

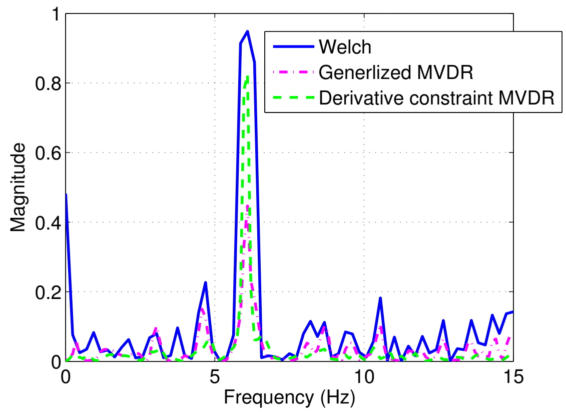

Fig. 4. MSC function of $\gamma^2_{x_1x_2}$.

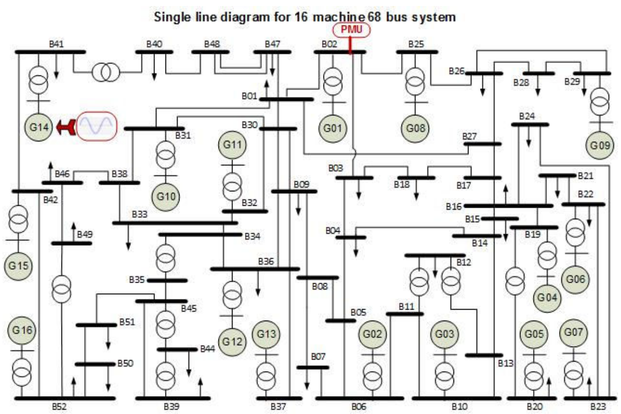

Fig. 5. Single line diagram of the 16-machine, 68-bus system.

of the Generalized MVDR method and the derivative constrained MVDR method is $K = 256, L = 65$. Their coherence spectra are plotted in Figs. 1-4, respectively. As it can be seen, oscillations can be detected by visually inspecting the coherence spectra on the heat maps. The Welch's method has a wide peak, which indicates that its frequency resolution is low. The problem with the MVDR is that there are some "blind spots" which can incur missing detection when oscillations happen in these frequencies. In contrast, the new method has no "blind spot" in the estimated MSC, and the narrow peaks indicate that the method retains the high frequency resolution. In addition, the lower magnitude at all other frequencies except the oscillation frequency indicates lower rate of false alarm.

4.2. Case study using the 16-machine model

To show the applicability of the proposed method in power systems, the 16-machine model illustrated in Fig. 5 is used. We use Power System Toolbox [21] to generate 60 minutes of simulation data.

To consider the effects of random load changes, 5% Gaussian white noise is added to the load buses. To mimic force oscillation in power system, the exciter voltage reference of generator 14 is modulated with a sinusoidal signal of 13.125Hz from the 10^{th} minute to 30^{th} minute and with a chirp signal of 12 to 14Hz from the 35^{th} minute to 55^{th} minute. A PMU is located at bus 2 and records the

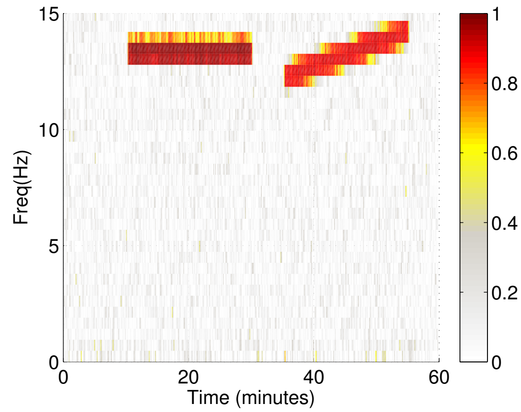

Fig. 6. MSC function estimated by the Welch's method.

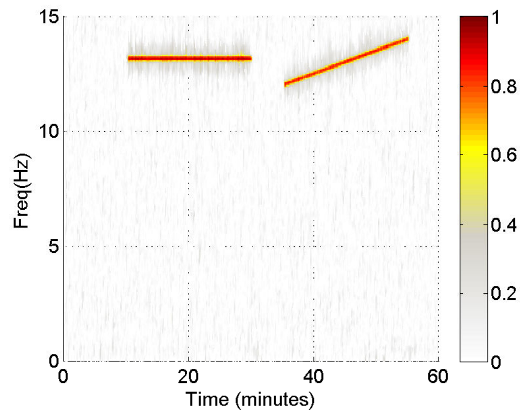

Fig. 7. MSC function estimated by the proposed MVDR method with derivative constraints.

real power from bus 2 to bus 53 at 60 samples/s. To remove the direct current components, we applied a first-order high-pass Butterworth filter with cutoff frequency of 0.01Hz.

With the same set up as in Section 4.1, we simulate the Welch's method and the proposed MVDR method with derivative constraint for oscillation detection. As shown in Figs. 6 and 7, both methods can successfully detect the oscillations. However, the proposed method has a narrower peak at the oscillation frequency, which indicates higher frequency resolution.

5. CONCLUSIONS

In this paper, a new MVDR method with a derivative constraint is proposed to detect the oscillations in power systems. The proposed method extends the original MVDR method by using the derivative constraint to both increase the estimation accuracy and remove the "blind spots". Simulations are conducted to demonstrate that the proposed method can avoid the "blind spots" problem and thus increase the oscillation detection accuracy.

6. REFERENCES

[1] G. Rogers, *Power System Oscillations*, Kluwer Academic Publishers, Boston, 2000.

[2] D. N. Kosterev, C. W. Taylor, and W. A. Mittelstadt, “Model validation for the August 10, 1996 WSCC system outage,” *IEEE Trans. Power Syst.*, vol. 14, no. 3, pp. 967–979, Aug. 1999.

[3] M. A. Magdy and F. Coowar, “Frequency domain analysis of power system forced oscillations,” *IEE Proceeding on Generation, Transmission and Distribution*, vol. 137, no. 4, pp. 261-268, Jul. 1990.

[4] D. J. Trudnowski and J. W. Pierre, “Overview of algorithms for estimating swing modes from measured responses,” *Proc. IEEE Power Eng. Soc. General Meeting*, pp. 18, Jul. 26-30, 2009.

[5] C. D. Vournas, N. Krassas, and B. C. Papadias, “Analysis of forced oscillations in a multi-machine power system,” *International Conference on control 91*, pp. 443-448, IET, 1991.

[6] M. Ghorbaniparvar, “A survey on forced oscillations in power system,” *Journal of Modern Power Systems and Clear Energy*, 2016.

[7] J. Van Ness, “Response of large power systems to cyclic load variations,” *IEEE Trans. on Power Apparatus and Systems*, vol. PAS-85, no. 7, pp. 723-727, 1966.

[8] J. Ma, P. Zhang, H. Fu, B. Bo, and Z. Dong, “Application of phasor measurement unit on locating disturbance source for low-frequency oscillation,” *IEEE Trans. Smart Grid*, vol. 1, no. 3, pp. 340-346, Dec. 2010.

[9] L. Chen, Y. Min, and W. Hu, “An energy-based method for location of power system oscillation source,” *IEEE Trans. on Power Systems*, vol. 28, pp. 828–836, May 2013.

[10] J. Follum and W. Pierre, “Initial results in the detection and estimation of forced oscillations in power systems,” *North American Power Symposium (NAPS)*, pp.1–6, Sept. 22–24, 2013.

[11] N. Zhou, “A coherence method for detecting and analyzing oscillations,” *2013 IEEE PES General Meeting*, Vancouver, BC, Canada, Jul. 21-25, 2013.

[12] N. Zhou and J. Dagle “Initial result in using self-coherence method for detecting sustained oscillation,” *IEEE Trans. on Power Systems*, vol. 5, pp. 1–9, May 2014.

[13] M. Ghorbaniparvar and N. Zhou, “Bootstrap-based hypothesis test for detecting sustained oscillations,” *Proc. IEEE Power Eng. Soc. General Meeting*, Jul. 26-30, 2015.

[14] N. Zhou, “A cross-coherence method for detecting oscillations,” *IEEE Trans. on Power Systems*, in press, 2016.

[15] S. M. Kay, *Fundamentals of Statistical signal processing, Volume 2: Detection theory*, Prentice Hall PTR, 1998.

[16] L. L. Scharf and L. T. Thomas, “Wiener filters in canonical coordinates for transform coding, filtering, and quantizing,” *IEEE Trans. on Signal Processing*, vol. 46, pp. 647–654, Mar. 1998.

[17] P. D. Welch, “The use of fast Fourier transform for the estimation of power spectra: A method based on time averaging over short, modified periodograms,” *IEEE Trans. Audio Electroacoust.*, vol. AU–15, no. 2, pp. 70–73, Jun. 1967.

[18] H. Zhao, S. Lu, R. Zou, K. Ju, and K. H. Chon, “Estimation of time-varying coherence function using time-varying transfer functions,” *Ann. Biomed. Eng.*, vol. 33, no. 11, pp. 1582–1594, Nov. 2005.

[19] J. Benesty, J. Chen, and Y. Huang, “A generalized MVDR spectrum,” *IEEE Signal Process. Lett.*, vol. 12, no. 12, pp. 827–830, Dec. 2005.

[20] P. Stoica and R. L. Moses, *Introduction to Spectral Analysis*. Upper Saddle River, NJ, USA: Prentice Hall, 1997.

[21] J. H. Chow and K. W. Cheung, “A toolbox for power system dynamics and control engineering education and research,” *IEEE Trans. on Power Systems.*, vol. 7, no. 4, pp. 1559-1564, Nov. 1992.